Magnetic properties of ion implanted $Ge_{1-x}Mn_x$ thin films solidified through pulsed laser melting

Melissa Commisso Dolph,[1,a)] Taeseok Kim,[2] Wenjing Yin,[3] Daniel Recht,[2] Wenbin Fan,[3] Jiani Yu,[3] Michael J. Aziz,[2] Jiwei Lu,[3] and Stuart A. Wolf[1,3]
[1]*Department of Physics, University of Virginia, Charlottesville, Virginia 22904, USA*
[2]*Harvard School of Engineering and Applied Sciences, Harvard University, Cambridge, Massachusetts 02138, USA*
[3]*Department of Materials Science and Engineering, University of Virginia, Charlottesville, Virginia 22904, USA*

(Received 31 January 2011; accepted 9 April 2011; published online 13 May 2011)

$Ge_{1-x}Mn_x$ thin films with an average Mn concentration of 0.64 at. % were fabricated through Mn ion implantation into crystalline germanium-on-insulator wafers. Implantation damage was removed and crystallinity restored by pulsed laser melting from a single 30-ns 308-nm $XeCl^+$ excimer laser pulse. Resolidified films demonstrated higher Curie temperatures but smaller saturation magnetizations than those of both as-implanted films and implanted films subjected to rapid thermal annealing. These findings are attributed to the redistribution of Mn during solidification. © *2011 American Institute of Physics*. [doi:10.1063/1.3590137]

I. INTRODUCTION

Diluted magnetic semiconductor (DMS) systems have garnered enhanced interest over the past decade because of their potential uses in spintronics.[1] A key property exhibited by DMS systems is carrier-mediated ferromagnetism. This has been observed in the most widely studied DMS materials.[2–4] With carrier-mediated ferromagnetism, one has the ability to control magnetic interactions by controlling the carrier concentration, which can be done either through co-doping or through the application of electric fields.

$Ge_{1-x}Mn_x$ is the DMS studied in this work. Ge has a higher hole mobility than Si or GaAs, which is a favorable property for a hole-mediated ferromagnetic system. $Ge_{1-x}Mn_x$ has also been found to exhibit ferromagnetism above room temperature with a Mn concentration as low as 0.25% (Ref. 5). Similar to work on (In,Mn)As (Ref. 3), the ferromagnetism in crystalline $Ge_{1-x}Mn_x$ thin films grown by molecular beam expitaxy (MBE) has been manipulated through the application of electric fields, but at temperatures well below room temperature.[4] In a recent report suggesting that the Curie temperature (T_C) can be considerably increased with increased geometrical confinement, electric field control over the ferromagnetism was also demonstrated in gated $Ge_{0.95}Mn_{0.05}$ quantum dots grown by MBE.[6] Such findings are promising for both spintronics and nanomagnetics.[7] As $Ge_{1-x}Mn_x$ remains an actively investigated DMS, further studies on MBE grown $Ge_{1-x}Mn_x$ have demonstrated the ability to synthesize nanocolumns which could be used as magnetic wires embedded in a semiconductor.[8–10] There is also continued interest in the influence of the substrate temperature on the structural and magnetic properties of both MBE-grown and ion implanted $Ge_{1-x}Mn_x$ films.[11]

The ability of pulsed laser melting (PLM) to recover implantation damage in semiconductors has been known for three decades,[12] with most research focused on incorporating high concentrations of single-electron donors and acceptors into Si.[12,13] Impurities outside of Groups III, IV, and V, such as Mn, cannot be so readily trapped onto substitutional lattice sites using PLM with laser pulses of order ~10 ns in duration; instead they tend to segregate toward the surface.[12] More recently, ion implantation and PLM (II-PLM) were combined to synthesize $Ga_{1-x}Mn_xAs$ thin films which exhibited Curie temperatures and saturation magnetizations (M_{sat}) very near those observed in films grown by low temperature MBE that were thermally annealed.[14]

In this paper, we report investigations of the magnetic and transport properties in $Ge_{1-x}Mn_x$ on insulating substrates fabricated by II-PLM.

II. EXPERIMENTS

The purchased Germanium-on-insulator (GeOI) wafers utilized in these experiments were fabricated by wafer bonding a (100) Ge crystal to the oxidized surface of a (100) crystal Si substrate. The resulting Ge film had a thickness of 200 nm, and the 400 nm thick layer of SiO_2 was designed to isolate the transport properties of the Ge film from those of the underlying semiconducting substrate. Eliminating the substrate contribution from transport measurements is the main advantage of using GeOI instead of bulk Ge. Additionally, GeOI could facilitate anticipated future electric gating experiments. However, using GeOI instead of bulk Ge had consequences for laser melting and solidification as discussed below.

The GeOI films were made *p*-type through light (~10^{15}/cm^3) boron doping. The films were implanted with Mn^+ ions to doses of 1.8×10^{15} and $4.2 \times 10^{15}/cm^2$ at energies of 170 and 60 keV, respectively. This combination of implantation doses and energies was expected to yield an average Mn concentration of 0.64% over the 200 nm film, a peak concentration of 2.1% at a depth of ~30 nm from the surface, and a

a)Electronic mail: mac5cx@virginia.edu.

monocrystalline un-implanted region at the Ge/SiO_2 interface.[15] All implantations were performed with active platen heating to 75 °C; beam heating was monitored to keep the substrate temperature within 10 °C of this set point, as substrate temperatures above 85 °C during MBE growth of $Ge_{1-x}Mn_x$ were reported to result in the formation of precipitates such as Ge_3Mn_5 and $Ge_{11}Mn_8$ (Ref. 16). Mn implantation into bulk Ge at temperatures of 240 °C or higher has also been found to result in the formation of precipitates.[17–19] These compounds exhibit ferromagnetism near room temperature,[20–22] but are neither carrier-mediated magnetic phases nor contributors to the global magnetism and are therefore undesirable for our purposes.

After Mn implantation, each sample was melted by a single 30 ns full width at half maximum pulse from a 308 nm $XeCl^+$ excimer laser, using fluences ranging from 0.22 to 0.46 J/cm^2 within a laser spot size of roughly 3×3 mm^2. An optical homogenizer reduced the standard deviation of the fluence to roughly 4% of the reported values over the entire laser spot. The fluence determined the melt depth, which was targeted to reach the crystalline seed layer in order for the film to resolidify as a single crystal. Time-resolved reflectivity using a 488 nm continuous wave Argon ion laser was employed to measure each sample's melt duration. Melt durations ranged between 100 and 200 ns for the fluences used.

Both x-ray diffraction (XRD) and electron diffraction (ED) were used to characterize the crystalline structure of the resolidified $Ge_{1-x}Mn_x$ films. A super-conducting quantum interference device vibrating sample magnetometer (SQUID VSM, Quantum Design Inc.) was used to measure the magnetization of the laser melted samples as a function of applied field and temperature. Hall and resistivity measurements were performed in a physical property measurement system (PPMS 6000, Quantum Design Inc.). Secondary ion mass spectrometry (SIMS) depth profiling was used to compare the Mn concentration depth profiles before and after PLM. Selected samples melted at the optimum fluence were prepared for transmission electron microscopy (TEM).

III. RESULTS AND DISCUSSION

A bright-field TEM image of an as-implanted sample is shown in Fig. 1. The corresponding ED pattern when the implanted region was in the selected area is shown in the inset. Implantation damage resulted in an amorphized Ge layer of roughly 180 nm, while an un-damaged monocrystalline layer roughly 20 nm thick remained at the Ge/SiO_2 interface. During PLM, the presence of this monocrystalline seed layer is necessary for the melt to solidify as a single crystal.

After Mn implantation, there is some evidence of surface roughness and indentation. However, TEM did not reveal the porous cavities associated with swelling that were observed in other studies on Mn implantation into Ge at similar substrate temperatures but more than thrice the Mn dose (2×10^{16} Mn/cm^2).[23,24] The absence of such structures in our specimens is reasonably consistent with the results of a recent study on Ge self-ion implantation at room temperature, which revealed that doses below 5×10^{15} Ge/cm^2 did not result in observable pores.[25]

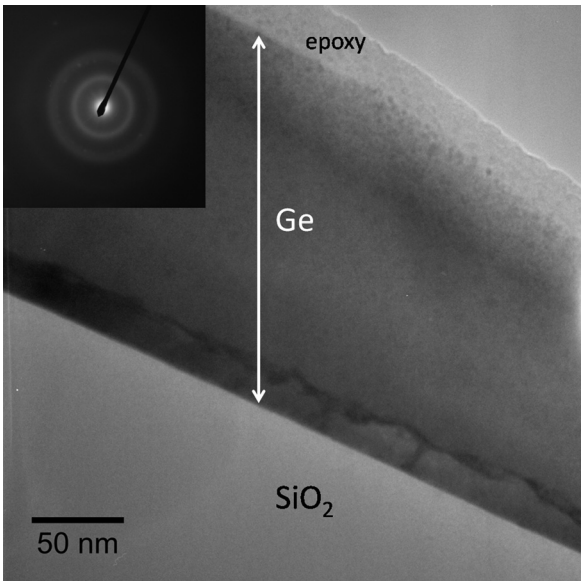

FIG. 1. Bright-field TEM image of as-implanted $Ge_{1-x}Mn_x$ material. Inset: amorphous structure revealed from ED pattern when implanted region was in the selected area.

Figure 2 shows XRD patterns from various Ge films. Shown are θ–2θ scans corresponding to samples of un-implanted GeOI (referred to as "as-received"), as-implanted $Ge_{1-x}Mn_x$, and laser melted $Ge_{1-x}Mn_x$. In as-received GeOI, a (400) Ge peak was present at ~66°. This peak was no longer visible after Mn implantation, suggesting that most, but not necessarily all, of the film became amorphous after implantation. For samples melted with fluences of 0.22, 0.24, and 0.27 J/cm^2 the (400) Ge peak returned, indicating that these fluences were successful at restoring the crystallinity of the $Ge_{1-x}Mn_x$ films with the same lattice orientation as the seed layer. Higher fluences presumably melted the entire seed layer and led to polycrystalline solidification.

Samples melted at fluences of 0.22, 0.24, or 0.27 J/cm^2, hereafter referred to as the "optimum fluences," were further

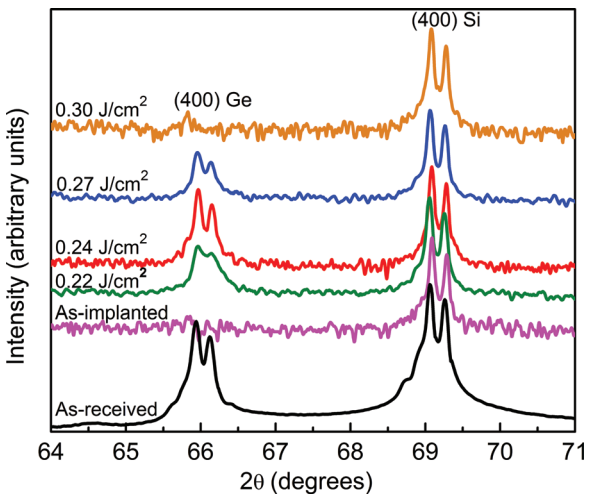

FIG. 2. (Color online) θ–2θ scans corresponding to (from bottom up): as-received GeOI, as-implanted $Ge_{1-x}Mn_x$, and $Ge_{1-x}Mn_x$ films melted with fluences of 0.22, 0.24, 0.27 and 0.30 J/cm^2. The peak near $2\theta = 66°$ corresponds to (400) Ge and the peak near 69.2° corresponds to the Si substrate. Double peaks were due to the presence of Cu $K\alpha_1$ and $K\alpha_2$ radiation in the x-ray.

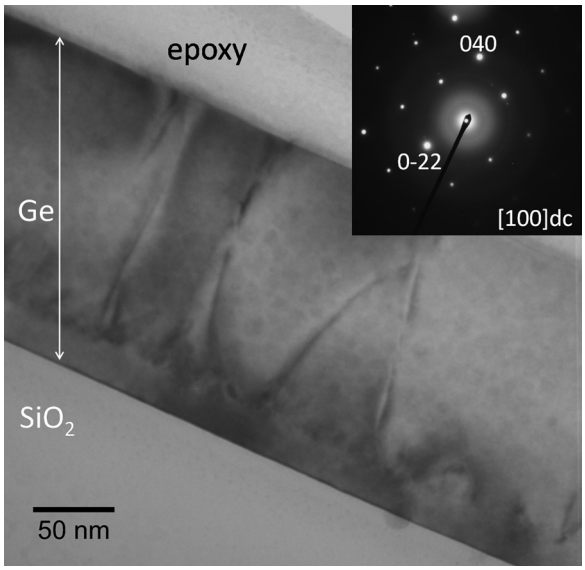

FIG. 3. TEM image along with the ED pattern (inset) for a sample melted with a laser beam fluence of 0.24 J/cm^2. Bright spots in the ED pattern correspond to (100) diamond cubic crystalline structure.

tested for single crystalline structure through electron backscatter diffraction (EBSD) carried out in a scanning electron microscope (SEM). One sample from each optimum fluence value was tested, and each was found to be single crystalline (not shown).

Figure 3 shows a TEM image of a sample melted at 0.24 J/cm^2 with the corresponding ED pattern shown in the inset. When the entire $Ge_{1-x}Mn_x$ film was in the selected area, ED revealed a single crystal (100) diamond cubic diffraction pattern, whereas amorphous rings dominated the diffraction pattern when as-implanted films were imaged (see Fig. 1 inset). Neither electron nor x-ray diffraction techniques revealed any evidence that secondary phases were present in the laser melted samples.

SIMS depth profiling was performed on a sample melted at an optimum fluence of 0.22 J/cm^2 and an as-implanted sample. The resulting Mn concentration-depth profiles are shown in Fig. 4. The Mn profile for the as-implanted film closely matches the simulated implantation profile.[15] The Mn distribution in the laser melted film is much less uniform

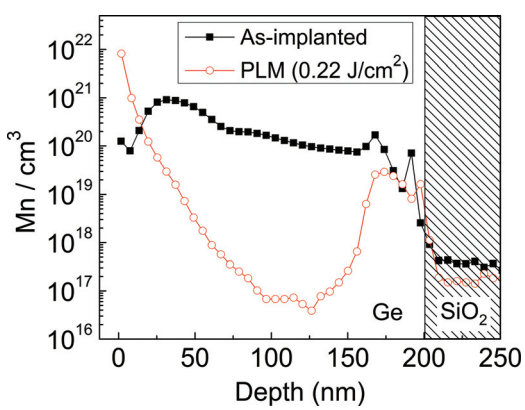

FIG. 4. (Color online) Mn concentration-depth profiles for as-implanted and laser melted (0.22 J/cm^2) samples. A significant fraction of the Mn segregated toward the surface of the film during laser melting and resolidification.

than that of the as-implanted film, with an enhanced Mn concentration near the surface and a diminished Mn concentration in the middle portion of the film. We interpret this profile to indicate that the laser pulse melted to a depth of ~170 nm and that the melt subsequently underwent epitaxial plane-front solidification starting at the crystalline seed layer, with the solidification front pushing the Mn substantially toward the surface. This scenario is consistent with previous observations after PLM for several transition metal impurities in Si.[12]

The general trends in the Mn depth profiles obtained from SIMS are more reliable than the obtained numerical values because the first several data points include artifacts of SIMS surface transients. For the laser melted sample these artifacts make it difficult to obtain an accurate value for the retained Mn dose. In the laser melted sample, the majority of the Mn resides at or very near the surface, as indicated by the first two circular data points in the depth profile, where the recorded values are the least reliable. Moreover, the very first, and least accurate, SIMS data point indicates an order of magnitude higher Mn concentration than its successor, which in turn indicates half an order of magnitude higher Mn concentration than its successor. Nevertheless, the nominal Mn doses were calculated by both histogram and trapezoidal integrations of the SIMS depth profiles. The histogram integration method yielded retained doses of 5.0×10^{15} and 5.9×10^{15} Mn/cm^2, in the as-implanted and PLM material, respectively, while the trapezoidal method yielded retained doses of 5.0×10^{15} and 3.7×10^{15} Mn/cm^2, respectively. We envisage no physical mechanism leading to a higher Mn dose in the laser melted material than in the as-implanted material, as is indicated by the histogram integration, and so we attribute this discrepancy to the error introduced by the surface transient. A ~30% loss of Mn, as indicated by the trapezoidal integration, is physically plausible and could be due to Mn evaporation during PLM. The retained doses obtained by the trapezoidal integration correspond to average Mn concentrations over the 200 nm film of 2.5×10^{20} and 1.8×10^{20} Mn/cm^3 for as-implanted and PLM material, respectively.

The magnetic behavior of a sample melted at 0.22 J/cm^2 can be seen in Fig. 5. A T_C of 25 K was estimated from the x-intercept of a line fit to the steepest slope of the remanence versus temperature curve shown in the main panel. The inset of Fig. 5 shows the magnetic moment for the same sample as a function of applied magnetic field at 5 K. Hysteresis was observed at measurement temperatures of 5, 10, and 15 K and disappeared by 50 K. The T_C of the laser melted films is well below the T_C of the most stable intermetallic Ge_yMn_x precipitates (Ge_3Mn_5 $T_C \approx 296$ K, $Ge_{11}Mn_8$ $T_C \approx 274$ K),[20–22] so in the unlikely case that these secondary phases were present, their contribution did not dominate the magnetic signals detected.

Hall and sheet resistance measurements were performed on a sample melted with 0.27 J/cm^2. In the Hall configuration, the ordinary Hall effect dominated the detected signals. The zero-field resistivity was determined by the Van der Pauw method and was found to increase with decreasing temperature, consistent with semiconducting behavior.

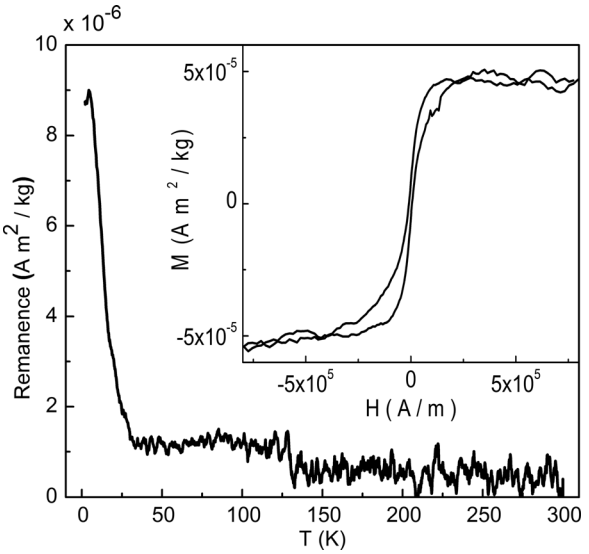

FIG. 5. Magnetization of a sample laser melted at 0.22 J/cm^2. The remanent magnetization is presented in the main panel. For this measurement, the sample was cooled down to 2 K in a field of 1 T, the magnetic field was removed, and the remanent magnetization was measured during warming to 300 K. A T_C of $\sim$25 K was determined from this plot. The hysteresis loop at 5 K is shown in the inset.

These points are illustrated in Fig. 6, which compares the magnetic and transport data of samples starting with the same Mn implantation conditions and treated differently. In addition to the data for as-implanted samples and samples melted at an optimum fluence, data are shown for implanted samples that underwent a rapid thermal anneal (RTA) at 300 °C for one min in forming gas (95% N_2 or Ar, 5% H_2) with no PLM treatment. As reported elsewhere,[26] this RTA condition has consistently been found to yield the largest saturation magnetization compared to as-implanted material and implanted material that underwent an RTA at 400 or 500 °C. However, performing an RTA at 300 °C has not been found to significantly restore the crystalline structure which was damaged during Mn implantation. Higher temperature rapid thermal anneals (at 400 or 500 °C) can lead to polycrystallinity in these ion implanted $Ge_{1-x}Mn_x$ films.[26] Further details and discussion on the ion implanted, RTA treated $Ge_{1-x}Mn_x$ systems are available in Ref. 26.

Figure 6(a) compares the zero-field temperature-dependent resistivity for as-implanted, laser melted (0.27 J/cm^2), and RTA-treated samples assuming a thickness of 200 nm. Figure 6(b) compares the Hall data for the same sample types at 5 K. The ordinary Hall effect dominates in all three cases. The sheet carrier concentrations were determined from the Hall slope after any contribution from magnetoresistance was subtracted out.[27] The sheet carrier concentrations were found to be 9.4×10^{13}, 2.4×10^{13}, and 1.2×10^{14} holes/cm^2 for as-implanted, laser melted, and RTA-treated material. Assuming the holes were distributed uniformly within a film of thickness 200 nm, the 3D hole concentrations would be 4.7×10^{18}, 1.2×10^{18}, and 5.8×10^{18} holes/cm^3, respectively. The laser melted films have slightly fewer activated carriers and a higher resistivity than as-implanted or RTA-treated films, but with the SIMS accuracy limitations discussed above, we cannot compare quantitatively the activation ratio of as-implanted and laser melted samples.

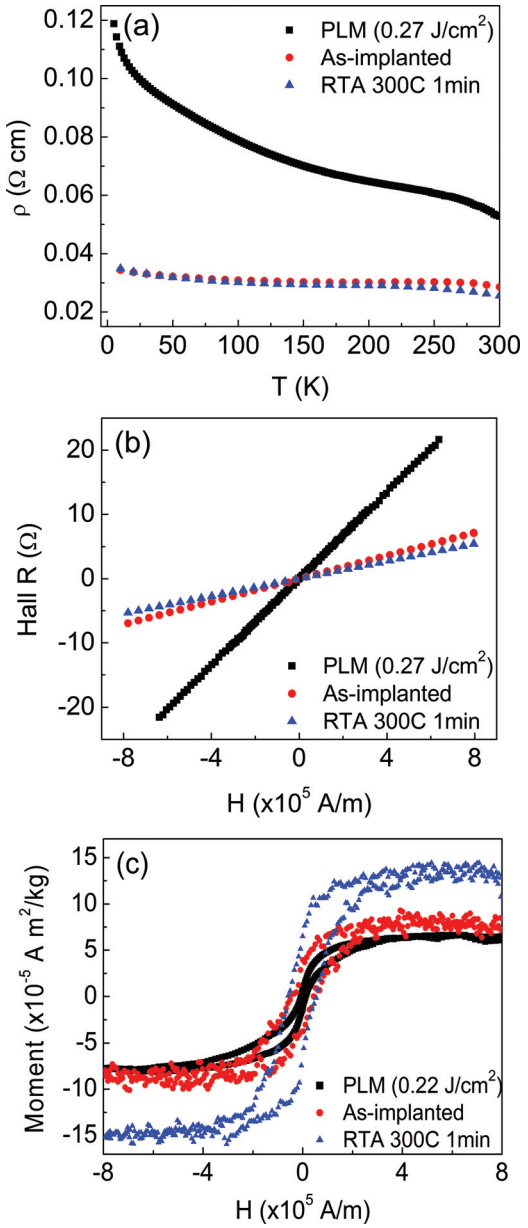

FIG. 6. (Color online) Comparison of samples with identical Mn implants and treated differently. (a) zero-field resistivity vs temperature (resistivity of as-received GeOI was 7 Ω · cm at 300 K). (b) Hall resistance at 5 K vs field; (c) magnetic moment at 5 K vs field.

It has been suggested that the hole concentration is a critical parameter for obtaining magnetotransport properties that can be correlated to the magnetization more directly observed by magnetometry in Mn-doped Ge.[28] Similar arguments were made for $Ga_{1-x}Mn_xAs$.[29] Our findings further support this suggestion, given that the 3D hole concentrations for the as-implanted, laser melted, and RTA-treated films in our study ($\sim 10^{18}$ holes/cm^3) were below the suggested threshold value (3×10^{19} holes/cm^3)[28,29] needed in order to obtain correlated magnetotransport and magnetization. This could explain the absence of an anomalous Hall effect and the dominance of the ordinary Hall effect even at low fields.

Figure 6(c) compares the field-dependent magnetic moment at 5 K of as-implanted, laser melted (0.22 J/cm^2), and RTA-treated samples. Although the T_C of the laser melted samples (~25 K) was roughly twice the T_C observed for as-implanted and RTA-treated films (~12 and 15 K, respectively), M_{sat} at 5 K decreased after PLM to 0.8 times M_{sat} for as-implanted films. Changes in M_{sat} can be used to estimate changes in the amount of ferromagnetically active ions present in a DMS system. In more conventional units, M_{sat} at 5 K for the as-implanted, laser melted, and RTA-treated samples shown in Fig. 6(c) are 0.18, 0.14, and 0.31 μ_B/Mn, respectively, assuming all of the implanted Mn contributes to the ferromagnetism. In comparison to the expected moment of three μ_B/Mn,[4,30] a value predicted by Ge *p* and Mn *d* hybridization which itself is still a topic of interest,[31] these values suggest that only 6–10% of the implanted Mn are ferromagnetically active. These values for the total magnetic moment fall within the wide range of values reported for $Ge_{1-x}Mn_x$ in the literature,[4–6,9,16,28,32] and comparable values (0.2−0.5 μ_B/Mn) were observed in flash-lamp annealed and amorphous $Ge_{1-x}Mn_x$ films with Mn concentrations ranging from 6 – 20 at. %.[28,32] In our experiments, one possible explanation for the decrease of M_{sat} after PLM is that there was some degree of antiferromagnetic coupling between Mn ions near the surface of the film as a result of the enhanced Mn concentration in this region. Another is that kinetic effects led fewer Mn atoms to occupy acceptor configurations during the rapid resolidification following PLM. A third is that the high surface concentration of Mn is in an inactive form, e.g., within a surface oxide rather than within the semiconductor itself.

The trends between PLM and thermal annealing seem to be different for $Ge_{1-x}Mn_x$ and $Ga_{1-x}Mn_xAs$. Scarpulla *et al.*[14] found that II-PLM could be used to produce a $Ga_{1-x}Mn_xAs$ system similar to those produced by low temperature MBE plus a thermal anneal. Our findings for $Ge_{1-x}Mn_x$ show that performing a RTA at 300 °C for one minute did produce a larger M_{sat} and a slightly higher hole concentration compared to as-implanted films, while PLM lowered the value of M_{sat}, increased the resistivity, and resulted in a slightly smaller hole concentration. The PLM treatment reported here is unusual, however, in that a thermally insulating oxide layer lies below the solidifying film and slows down the solidification rates considerably compared to rates that one might encounter in PLM of bulk semiconductors. Slow solidification rates are known to inhibit solute trapping and thereby to enhance segregation to the free surface.[13]

While this manuscript was being prepared, Zhou *et al.*[33] reported the observation of carrier-mediated ferromagnetism in Mn-implanted Ge created by II-PLM. They found that their fabrication procedure yielded precipitates plus crystalline $Ge_{1-x}Mn_x$ with x = "a few percent," and an attainable hole concentration large enough to give rise to an AHE that mimicked the magnetic moment at 5 K. Their results show that II-PLM under the right conditions can be used to create a $Ge_{1-x}Mn_x$ system with favorable magnetotransport properties at low temperatures. There are several significant differences between the experimental procedure and results reported here and those reported by Zhou *et al.*: (i) Zhou *et al.* implanted an average of ten at. % Mn, which is more than an order of magnitude more than our implanted average of 0.6 at. %; (ii) Zhou *et al.* performed PLM on bulk Ge whereas our PLM treatment was on GeOI; (iii) Zhou *et al.* used a pulsed laser with unusual characteristics (300 ns, 2 mm × 0.040 mm scanned stripe with frequency 50 kHz), in particular a pulse duration an order of magnitude longer than ours. Although we are unable to estimate the solidification rate resulting from their particular PLM treatment, we expect that longer pulse durations normally slow resolidification, impede solute trapping and enhance segregation to the surface.[13] Consequently, we might have expected our PLM procedure to trap a higher fraction of the implanted Mn than Zhou's. However, the presence of the buried oxide below our surface Ge layers cut our solidification rates by an estimated factor of five, from ~5 m/s to ~1 m/s according to numerical solutions of the heat equation. Despite the longer pulse duration, Zhou *et al.* were able to retain more Mn throughout the implanted region through some combination of implanting more Mn and PLM processing without the buried oxide. If this is correct, we should expect even higher trapped Mn concentrations from higher dose implants and PLM with shorter laser pulses on bulk Ge substrates.

Even though Zhou *et al.* were able to trap more Mn than we were, the temperature at which the magnetotransport and direct ferromagnetic responses diverged (7.5 K) in their $Ge_{1-x}Mn_x$ system was well below the temperature at which ferromagnetic hysteresis was lost (~100 K) as determined from their direct magnetic measurements. This differs from the trends observed in $Ga_{1-x}Mn_xAs$,[14] where the magnetotransport and magnetic results mimicked each other for a much larger temperature range, persisting close to T_C. Hence, even if further refinements of PLM-based synthesis methods are successful at increasing attainable Mn supersaturations in single-crystal Ge, it is not yet clear whether II-PLM can be used to produce $Ge_{1-x}Mn_x$ alloys with robust magnetotransport persisting to room temperature or even to temperatures near T_C.

IV. SUMMARY

We have synthesized precipitate free, single crystal $Ge_{1-x}Mn_x$ thin films on GeOI through II-PLM and characterized their crystalline structure, magnetic signature, and electrical transport behavior. PLM fluences ranging from 0.22 to 0.27 J/cm^2 restored the crystallinity of the $Ge_{1-x}Mn_x$ films after they had been amorphized by ion implantation. After ion implantation, PLM increased T_C from ~15 K to 25 K but the sheet resistance increased after PLM and the saturation magnetization actually decreased after PLM. SIMS depth profiling indicated that a large fraction of the Mn segregated toward the surface of the films during resolidification. The large amount of segregation was attributed to the roughly fivefold decrease in solidification velocity caused by the thermal bottleneck of the underlying SiO_2.

ACKNOWLEDGMENTS

The authors thank Dr. Cindi Dennis at NIST Gaithersburg for her assistance using the VSM SQUID and we also thank Dr. Li He for useful discussions on previously studied ion

implanted GeMn systems and TEM. This work was supported by the NRI and NSF (Grant No. DMR-0080016) and the Virginia Center for Innovative Technology (VCIT). Research at Harvard was supported in part by NSF (Grant No. ECCS-0701417). D. Recht was supported in part by the Department of Defense (DoD) through the National Defense Science & Engineering Graduate Fellowship (NDSEG) Program.

[1]S. A. Wolf, D. D. Awschalom, R. A. Buhrman, J. M. Daughton, S. von Molnar, M. L. Roukes, A. Y. Chtchelkanova, and D. M. Treger, Science **294**, 1488 (2001).
[2]H. Ohno, Science **281**, 951 (1998)
[3]H. Ohno, D. Chiba, F. Matsukura, T. Omiya, E. Abe, T. Dietl, Y. Ohno, and K. Ohtani, Nature **408**, 944 (2000).
[4]Y. D. Park, A. T. Hanbicki, S. C. Erwin, C. S. Hellberg, J. M. Sullivan, J. E. Mattson, T. F. Ambrose, A. Wilson, G. Spanos, and B. T. Jonker, Science **295**, 651 (2002).
[5]C. G. Zeng, Z. Y. Zhang, K. van Benthem, M. F. Chisholm, and H. H. Weitering, Phys. Rev. Lett. **100**, 066101 (2008).
[6]F. Xiu, Y. Wang, J. Kim, A. Hong, J. Tang, A. P. Jacob, J. Zou, and K. L. Wang, Nat. Mater. **9**, 337 (2010).
[7]S. A. Wolf, J. Lu, M. R. Stan, E. Chen, and D. Treger, Proc. IEEE **98**, 2155 (2010).
[8]I.-S. Yu, M. Jamet, T. Devillers, A. Barski, P. Bayle-Guillemaud, C. Beigne, J. Rothman, V. Baltz, and J. Cibert, Phys. Rev. B **82**, 035308 (2010).
[9]A. Jain, M. Jamet, A. Barski, T. Devillers, C. Prret, P. Bayle-Gullemaud, S. Gambardelli, V. Maurel, and G. Desfonds, Appl. Phys. Lett. **97**, 202502 (2010).
[10]D. Bougeard, N. Sircar, S. Ahlers, V. Lang, G. Abstreiter, A. Trampert, J. M. LeBeau, S. Stemmer, D. W. Saxey, and A. Cerezo, Nano Lett. **9**, 3743 (2009).
[11]R. Gunnella, L. Morresi, N. Pinto, A. Di Cicco, L. Ottaviano, M. Passacantando, A. Verna, G. Impellizzeri, A. Irrera, and F. d'Acapito, J. Phys.: Condens. Matter **22**, 216006 (2010).
[12]Laser Annealing of Semiconductors, edited by J. Poate and J. Mayer (Academic, New York, 1982).
[13]R. Reitano, P. M. Smith, and M. J. Aziz, J. Appl. Phys. **76**, 1518 (1994).
[14]M. A. Scarpulla, R. Farshchi, P. R. Stone, R. V. Chopdekar, K. M. Yu, Y. Suzuki, and O. D. Dubon, J. Appl. Phys. **103**, 073913 (2008).
[15]ProfileCode Software, Core Systems Inc., 1050 Kifer Road, Sunnyvale, CA 94086.
[16]A. P. Li, J. F. Wendelken, J. Shen, L. C. Feldman, J. R. Thompson, and H. H. Weitering, Phys. Rev. B **72**, 195205 (2005).
[17]M. Passacantando, L. Ottaviano, F. D'Orazio, F. Lucari, G. Impellizzeri and F. Priolo, Phys. Rev. B **73**, 195207 (2005).
[18]L. Ottaviano, M. Passacantando, S. Picozzi, A. Continenza, R. Gunnella, A. Verna, G. Bihlmaier, G. Impellizzeri, and F. Priolo, Appl. Phys. Lett. **88**, 061907 (2006).
[19]L. Ottaviano, M. Passacantando, A. Verna, R. Gunnella, E. Prencipi, A. Di Cicco, G. Impellizzeri, and F. Priolo, J. Appl. Phys. **100**, 063528 (2006).
[20]C. G. Zeng, S. C. Erwin, L. C. Feldman, A. P. Li, R. Jin, Y. Song, J. R. Thompson, and H. H. Weitering, Appl. Phys. Lett. **83**, 5002 (2003).
[21]N. Yamada, J. Phys. Soc. Jpn. **59**, 273 (1990).
[22]N. Yamada, K. Maeda, Y. Usami, and T. Ohoyama, J. Phys. Soc. Jpn. **55**, 3721 (1986).
[23]A. Verna, L. Ottaviano, M. Passacantando, S. Santucci, P. Picozzi, F. D'Orazio, F. Lucari, M. De Biase, R. Gunnella, M. Berti, A. Gasparotto, G. Impellizzeri, and F. Priolo, Phys. Rev. B **74**, 085204 (2006).
[24]L. Ottaviano, A. Verna, V. Grossi, P. Parisse, S. Piperno, M. Passacantando, G. Impellizzeri, and F. Priolo, Surf. Sci. **601**, 2623 (2007).
[25]L. Romano, G. Impellizzeri, M. V. Tomasello, F. Giannazzo, C. Spinella, and M. G. Grimaldi, J. Appl. Phys. **107**, 084314 (2010).
[26]W. Yin, L. He, M. C. Dolph, J. Lu, R. Hull, and S. A. Wolf, J. Appl. Phys. **108**, 093919 (2010).
[27]H. Ohno, H. Munekata, S. von Molnár, and L. L. Change, J. Appl. Phys. **69**, 6013 (1991).
[28]S. Zhou, D. Burger, W. Skorupa, P. Oesterlin, M. Helm, and H. Schimdt, Appl. Phys. Lett. **96**, 202105 (2010).
[29]S. U. Yuldashev, H. C. Jeon, H. S. Im, T. W. Kang, S. H. Lee, J. K. Furdyna, Phys. Rev. B **70**, 193203 (2004).
[30]A. Stroppa, S. Picozzi, A. Continenza, and A. J. Freeman, Phys. Rev. B **68**, 155203 (2003).
[31]A. Stroppa, G. Kresse, and A. Continenza, Phys. Rev. B **83**, 085201 (2011).
[32]L. Zeng, J. X. Cao, E. Helgren, J. Karel, E. Arenholz, L. Ouyang, D. J. Smith, R. Q. Wu, and F. Hellman, Phys. Rev. B **82**, 165202 (2010).
[33]S. Zhou, D. Burger, A. Mucklich, C. Baumgart, W. Skorupa, C. Timm, P. Oesterlin, M. Helm, and H. Schmidt, Phys. Rev. B **81**, 165204 (2010).